REDOUBT: Duo Safety Validation for Autonomous Vehicle Motion Planning

Shuguang Wang[1] **Qian Zhou**[1] **Kui Wu**[2] **Dapeng Wu**[1] **Wei-Bin Lee**[3] **Jianping Wang**[1]
[1]City University of Hong Kong, Hong Kong, China
[2]University of Victoria, B.C., Canada
[3]Information Security Center, Hon Hai Research Institute, Taipei, Taiwan
sgwang6-c@my.cityu.edu.hk
{qiazhou, jianwang}@cityu.edu.hk wkui@uvic.ca
dpwu@ieee.org wei-bin.lee@foxconn.com

Abstract

Safety validation, which assesses the safety of an autonomous system's motion planning decisions, is critical for the safe deployment of autonomous vehicles. Existing input validation techniques from other machine learning domains, such as image classification, face unique challenges in motion planning due to its contextual properties, including complex inputs and one-to-many mapping. Furthermore, current output validation methods in autonomous driving primarily focus on open-loop trajectory prediction, which is ill-suited for the closed-loop nature of motion planning. We introduce REDOUBT, the first systematic safety validation framework for autonomous vehicle motion planning that employs a duo mechanism, simultaneously inspecting input distributions and output uncertainty. REDOUBT identifies previously overlooked unsafe modes arising from the interplay of In-Distribution/Out-of-Distribution (OOD) scenarios and certain/uncertain planning decisions. We develop specialized solutions for both OOD detection via latent flow matching and decision uncertainty estimation via an energy-based approach. Our extensive experiments demonstrate that both modules outperform existing approaches, under both open-loop and closed-loop evaluation settings. Our codes are available at: `https://github.com/sgNicola/Redoubt`.

1 Introduction

Motion planning—the process of generating a trajectory for the ego-vehicle based on sensed traffic scenario data—is a cornerstone of autonomous driving. Learning-based motion planning methods [48, 54, 47, 45, 7], which leverage datasets of human driving behavior to train autonomous systems, have gained increasing attention due to their potential for greater adaptability compared to traditional rule-based approaches. Despite significant advances, autonomous vehicles continue to struggle with the full complexity of real-world driving scenarios [11, 29, 28, 42].

Safety validation for motion planning, which assesses whether a vehicle's decisions are safe in a given scenario, is thus critical. When an unsafe decision is detected, the validation module can: (1) immediately override the decision and initiate fallback measures (e.g., manual takeover [1]) to ensure short-term safety, and (2) flag the scenario as "challenging" to prioritize improvement in subsequent continual learning iterations [37, 41]. Safety validation could reduce or prevent tragedies like the March 29, 2025, Xiaomi SU7 incident, which resulted in three fatalities [12]. Nevertheless, such a systematic safety validation framework is currently lacking—a gap our this work seeks to address.

Safety validation can potentially be approached via two main angles: *input inspection* and *output inspection*. In the first category, *input inspection*, we draw inspiration from *Out-of-Distribution*

39th Conference on Neural Information Processing Systems (NeurIPS 2025).

(OOD) detection in other machine learning fields, such as image classification [49, 3], to establish a novel approach for assessing safety levels in autonomous driving. This approach determines whether a given input falls within the trained model's familiar data distribution: it is termed In-Distribution (InD) if it does, and otherwise Out-of-Distribution (OOD) [51]. In our context, if a traffic scenario is identified as OOD, the system could downgrade the safety score of the resulting decision. However, *input inspection* strategies based on OOD detection have not yet been used in motion planning, and adapting them poses unique challenges. Unlike classification tasks, motion planning requires predicting distributions over plausible future trajectories conditioned on complex, context-dependent inputs [52]. This one-to-many mapping obscures the underlying data distribution, making it difficult to define meaningful feature distances or confidence margins for OOD detection.

In the second category, *output inspection*, safety validation assesses the *uncertainty* of the autonomous system's output and deems those with high uncertainty as unsafe. However, these approaches are mainly designed for trajectory prediction rather than motion planning [35, 16]. In a nutshell, trajectory prediction predicts the future paths of other road agents, e.g., vehicles, pedestrians, and cyclists, based on their current/past behavior and environmental context, while motion planning determines the ego vehicle's own trajectory to navigate safely and efficiently toward a goal, considering predicted trajectories of others. Safety validation for trajectory prediction faces significant barriers when applied to motion planning. This is because trajectory prediction is typically validated in an open-loop setting [39, 36], where predicted trajectories of surrounding agents are compared against ground-truth logs from recorded datasets. In contrast, motion planning operates in a closed-loop manner: the ego-vehicle continuously uses feedback from its current state and the dynamic environment to update and adjust its plans in real time [17]. Consequently, applying existing *output inspection* approaches directly to motion planning could lead to critical failures, such as falsely certifying the ego vehicle's trajectory as safe when it actually results in collisions or road departures [10].

We propose **REDOUBT**, the first framework to systematically integrate *input inspection* through OOD detection and *output inspection* via uncertainty estimation for the safety validation of autonomous vehicle motion planning.

First, we develop specialized solutions for OOD scenario detection and uncertain decision estimation within the context of autonomous vehicle motion planning. We identify distributional shifts by estimating distribution likelihoods in the latent space using flow matching. Specifically, we employ a velocity field, enhanced with Gaussian Fourier Projection to capture temporal dynamics, to match target distributions and enable a principled estimation of distributional shifts in trajectory evolution. For estimating planning decision uncertainty under closed-loop dynamics, we introduce an energy-based approach that assigns risk-sensitive energy scores. These scores, computed based on future distances to obstacles or surrounding agents, provide a dense and continuous measure of safety risk, unlike sparse binary violation labels. During inference, we aggregate energy scores and trajectory probabilities to assess safety risks under closed-loop execution.

Moreover, REDOUBT employs a duo validation approach—simultaneously inspecting input distributions (traffic scenarios) and output uncertainty (planning decisions). The key insight behind this duo strategy, supported by our experiments, is that input and output validation are *complementary*, not interchangeable. By jointly validating both dimensions, it categorizes driving situations into four types: (a) **InD scenario + certain decision** → *Safe*, (b) **InD scenario + uncertain decision** → *Unsafe*, (c) **OOD scenario + certain decision** → *Unsafe*, and (d) **OOD scenario + uncertain decision** → *Unsafe*. Notably, REDOUBT uniquely identifies situations (b) and (c), which have been overlooked by existing approaches that rely solely on input or output inspection, thereby offering more comprehensive safety guarantees. In summary, our contributions are:

- We propose a novel duo safety validation approach for autonomous driving motion planning that concurrently inspects both input and output, revealing two previously overlooked unsafe situations.
- We design a latent flow matching method to estimate distributional shifts and detect OOD traffic scenarios, effectively modeling the multi-modal and dynamic nature of planning contexts.
- We present an energy-based risk prediction approach that integrates risk signals and trajectory probabilities to estimate driving decision uncertainty without requiring explicit violation labels.
- We outperform previous approaches on the nuPlan dataset in both OOD detection and decision uncertainty estimation. Our method demonstrates superior performance in both open-loop and closed-loop settings.

2 Related Work

Out-of-Distribution (OOD) Detection. OOD detection has been extensively studied in image classification [32, 53, 50] but remains underexplored in motion planning. Post-hoc methods such as Maximum Softmax Probability [19], MaxLogit [18], and energy-based scoring [34] derive OOD scores from the output layer of trained classifiers, offering simplicity and ease of implementation. Feature-space methods, including Mahalanobis distance [26] and k-Nearest Neighbor (KNN) approaches [40], estimate distributional deviation based on distances in the learned representation space. However, applying these methods to motion planning is challenging—post-hoc scores often yield overconfident predictions, while feature-space methods struggle with the one-to-many mapping and complex inputs, which obscure the data distribution.

Motion Planning. Motion planning aims to generate safe and efficient trajectories for autonomous agents. Hybrid methods, such as GC-PGP [10], integrate learning-based models with rule-based priors through centerline selection algorithms, achieving a balance between adaptability and safety. Fully learning-based models, including GameFormer [22] and PlanTF [8], leverage scene encoding to learn decision-making policies, generate multi-modal trajectory candidates, and select optimal plans based on trajectory probabilities and constraint satisfaction. Methods such as PLUTO [7] address distribution shift via contrastive learning, using data augmentations to shape latent representations. PlanScope [46] incorporates auxiliary losses based on Euclidean Signed Distance Fields (ESDF) to model cost and enforce safety constraints during planning. While these approaches have significantly advanced the performance of learning-based motion planning, they primarily overlook OOD detection.

Uncertainty Estimation. Uncertainty estimation in motion prediction has emerged as a valuable tool for safety validation of trajectory forecasts [36]. For example, Joodu [44] uses imitation error as a proxy for uncertainty, while Filos et al.[13] leverage disagreement among predicted trajectories to detect potential distribution shifts. DECODE [27] employs normalizing flows for domain awareness and selects the model with the highest likelihood to generate trajectory predictions. SOTIF [38] measures perceptual uncertainty with entropy, providing signals that guide risk evaluation in downstream motion prediction. Other works incorporate uncertainty arising from map inaccuracies and occlusions into trajectory prediction[16], and utilize trajectory distribution entropy to quantify predictive uncertainty [35]. Despite their utility, these uncertainty estimation approaches remain largely restricted to open-loop settings, relying on surrogate metrics such as imitation loss. These metrics fail to capture critical closed-loop risks—including collisions and road departures.

3 Methodology

This section introduces the REDOUBT framework, which consists of two key modules (dashed boxes in Figure 1): (1) an Out-of-Distribution (OOD) Detection module based on Flow Matching and (2) a Decision Uncertainty Estimation module. REDOUBT is orthogonal to and can be integrated with various existing motion planning solutions to validate the safety of their planned trajectories.

3.1 Learning-based Motion Planning

To begin, we outline the background of modern ML-based motion planning models. These models leverage scene encoders to transform multi-modal driving contexts into high-dimensional latent representations [23, 7], which encapsulate semantic and contextual information essential for trajectory prediction [25, 24, 33]. Formally, the driving context is encoded as a scene representation $\mathbf{x} = \{E_E, E_A, E_O, E_M\}$, where E_E denotes the ego vehicle state, E_A the states of dynamic agents, E_O static object features, and E_M map information. The model predicts future trajectories for dynamic agents, denoted as $Y_{1:N_d}^{1:T_f} = \{y_1^{1:T_f}, \ldots, y_{N_d}^{1:T_f}\}$. Furthermore, it generates a set of N_m multi-modal ego trajectories, represented as $Y_0^{1:T_f} = \{(y_{0,i}^{1:T_f}, p_i)\}_{i=1}^{N_m}$ where p_i is the probability associated with the i-th candidate trajectory. The final trajectory τ^* is selected by optimizing p_i while adhering to traffic-related constraints. Building on this, we propose a latent-space-driven framework for OOD detection and decision uncertainty estimation.

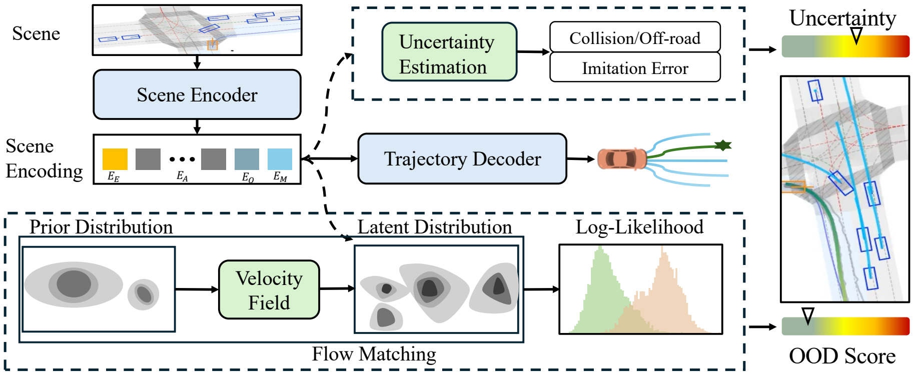

Figure 1: Overview of the proposed REDOUBT framework. The OOD Detection module utilizes Flow Matching to model the In-Distribution density of the latent space, learning a velocity field to transform the prior known distribution into the target distribution. The Decision Uncertainty Estimation module predicts collision and off-road violations, as well as imitation errors. The final decision-making process considers both the OOD score and the decision uncertainty.

3.2 OOD Detection based on Flow Matching

The OOD Detection module is designed to identify "unfamiliar" input scenarios and trigger a signal of potential danger. Similar to OOD detection approaches in other domains (e.g., [15, 53]), it can be described as employing a score function to determine whether a given input belongs to the In-Distribution (InD) or the Out-of-Distribution (OOD). We derive this score function from advancements in the generative AI field, applying it for safety validation. The core intuition is that generative models create a score to evaluate the similarity between the current distribution and the target distribution, guiding their path toward the target. Leveraging this concept in a novel way, we use the score to measure an input traffic scenario's proximity to the InD density.

Preliminary on Flow Matching. Flow Matching (FM) is a recently proposed paradigm for training generative models by transforming a simple source distribution into a target data distribution [30, 31, 9]. The aim of FM is to learn a time-dependent flow ϕ_t that continuously maps samples from a known source distribution, typically a standard Gaussian, to the target distribution [2]. This flow $\phi_t : [0,1] \times \mathbb{R}^d \to \mathbb{R}^d$ is defined by an ordinary differential equation (ODE) parameterized by a velocity field u_t:

$$\frac{\mathrm{d}\phi_t(\mathbf{x})}{\mathrm{d}t} = u_t(\phi_t(\mathbf{x})). \tag{1}$$

The time-dependent probability path $(p_t)_{0\leq t\leq 1}$, which smoothly interpolates between the source distribution $p_0 = p$ and the target distribution $p_1 = q$. A velocity field u_t is suggested to generate this probability path. To learn the velocity field, a neural network u_t^θ is used to approximate the target velocity field u_t. The parameters θ of the neural network are typically estimated by minimizing the following objective function:

$$\mathcal{L}_{FM}(\theta) = \mathbb{E}_{t\sim U[0,1],\mathbf{x}\sim p_t} \| u_t^\theta(\mathbf{x}) - u_t(\mathbf{x}) \|^2, \tag{2}$$

where $u_t(\mathbf{x})$ represents the target velocity field derived from the continuity equation.

Velocity Field. Let $\mathbf{z} \in \mathbb{R}^d$ represent the latent encoding of a motion planning trajectory obtained from the scene encoder. We define a time-dependent flow $\phi_t(\mathbf{z})$, governed by a neural velocity field u_t^θ, which evolves along an interpolation path from a known prior distribution p_0 to the target data distribution p_1. To incorporate the temporal dimension, we employ a Gaussian Fourier Projection to embed the scalar time t into a high-dimensional feature vector. The time embedding is given by:

$$\gamma(t) = [\sin(2\pi t W), \cos(2\pi t W)], \quad W \in \mathbb{R}^{d_t/2}, \tag{3}$$

where W is a projection matrix that encodes multi-frequency information. This time embedding is then processed by a residual Multi-Layer Perceptron (MLP) architecture.

The velocity field is trained using a velocity matching loss, which minimizes the discrepancy between the predicted flow velocity $u_t^\theta(\mathbf{z}_t)$ and the velocity $\frac{d\mathbf{z}_t}{dt}$ along the interpolation path. The loss function is given by:

$$\mathcal{L}_{\text{flow}} = \mathbb{E}_{t\sim U[0,1],(\mathbf{z}_0,\mathbf{z}_1)\sim\pi_{0,1}} \left[\left\| u_t^\theta(\mathbf{z}_t) - \frac{d\mathbf{z}_t}{dt} \right\|^2 \right], \tag{4}$$

where $\mathbf{z}_t$ is sampled along an interpolation path between $\mathbf{z}_0$ and $\mathbf{z}_1$, with velocity $\frac{d\mathbf{z}_t}{dt}$ along the path. Here, $\pi_{0,1}$ defines the joint distribution of $\mathbf{z}_0$ and $\mathbf{z}_1$, and the interpolation is guided by the Affine Probability Path under a Conditional Optimal Transport schedule [14].

Computing Log-Likelihood. Once the velocity field is trained, the log-likelihood of a sample $\mathbf{z}_1 \sim p_1$ can be computed by solving the flow ODE backward in time using an Euler solver. For the prior distribution p_0, we adopt a Gaussian Mixture Model (GMM) with N_m components to represent the multi-modal latent space. Using the Instantaneous Change of Variables formula [6], the log-likelihood of the target distribution is expressed as:

$$\log p_1(\mathbf{z}_1) = \log \left(\frac{1}{N_m} \sum_{i=1}^{N_m} \mathcal{N}(\mathbf{z}_0 \mid \boldsymbol{\mu}_i, \sigma_i^2\mathbf{I}) \right) - \int_0^1 \nabla \cdot u_t^\theta(\mathbf{z}_t)\, dt, \tag{5}$$

where $\mathcal{N}(\mathbf{z}_0 \mid \boldsymbol{\mu}_i, \sigma_i^2\mathbf{I})$ represents the i-th Gaussian component of the prior distribution, characterized by mean $\boldsymbol{\mu}_i$ and isotropic covariance matrix $\sigma_i^2\mathbf{I}$. The GMM contains N_m components, each with an equal mixture weight of $1/N_m$. The term, $-\int_0^1 \nabla \cdot u_t^\theta(\mathbf{z}_t)\, dt$, is the divergence integral, which quantifies the density evolution as the sample flows from $\mathbf{z}_1$ to $\mathbf{z}_0$ under the velocity field $u_t^\theta(\mathbf{z}_t)$.

3.3 Decision Uncertainty Estimation

The Decision Uncertainty Estimation module is a multi-output network designed to predict various uncertainty metrics for planned trajectories, encompassing both open-loop and closed-loop measures. First, in open-loop settings, uncertainty is represented by imitation error, often quantified using Average Displacement Error (ADE): ADE $= \frac{1}{T_f}\sum_{t=1}^{T_f} \|y_t - \hat{y}_t\|_2$, where y_t is the ground truth trajectory, and $\hat{y}_t$ is the predicted trajectory. Second, in closed-loop dynamics, uncertainty is indicated by two metrics: 1) No-Fault Collisions (NFC), which refer to collisions that could have been avoided with proper planning, and 2) Drivable Area Compliance (DAC), which assesses whether the ego vehicle operates within the mapped drivable area. Safety violations are represented as Boolean values (0: no violation, 1: violation). In the absence of violation labels during closed-loop no-feedback training, we propose a geometry-driven Violation Energy Score as pseudo-labels [43]. Leveraging signed distance as a physically intuitive metric, it transforms trajectories into continuous risk signals, capturing finer-grained risk features and addressing data scarcity in collision and driving area violation scenarios. The Violation Energy Score is further combined with trajectory probability to estimate decision uncertainty.

Violation Energy Score. At first, we construct the cost map using the Euclidean Signed Distance Field(ESDF) according to prior work [7, 54]. Non-drivable regions, such as obstacles and off-road areas, are rasterized into a binary mask. A distance transform is applied to compute a signed distance field, encoding the shortest distance of each pixel to the nearest obstacle or boundary. The vehicle is approximated as a set of N covering circles, each with a predefined radius R_c. Each point in the trajectory $\tau = \{y^t \mid t = 1, \ldots, T_f\}$ is projected onto the ESDF, where bilinear interpolation is used to calculate the signed distance d_i^t between the i-th covering circle at time t and the nearest semantic region. A penalty is applied when $d_i^t < R_c$, enforcing adherence to drivable area constraints.

The violation energy for a given trajectory is defined as:

$$E = \frac{1}{T_f} \sum_{t=1}^{T_f} \sum_{i=1}^{N} \mathbf{M}_i^t \cdot \varphi(d_i^t), \tag{6}$$

where T_f is the trajectory length, N is the number of covering circles, $\mathbf{M}_i^t$ is a binary mask indicating whether the i-th circle at time t intersects a region of interest (e.g., obstacles or boundaries), and $\varphi(d_i^t)$ is a penalty function quantifying the risk associated with the signed distance d_i^t.

To address different safety constraints, we define two penalty functions: $\varphi_{\text{nfc}}(d_i^t)$ for No at-fault Collisions (NFC) and $\varphi_{\text{dac}}(d_i^t)$ for Drivable Area Compliance (DAC). The NFC penalty is defined as:

$$\varphi_{\text{nfc}}(d_i^t) = \max(0, \exp(R_c - d_i^t) - 1), \tag{7}$$

which grows exponentially as d_i^t approaches or falls below R_c. This emphasizes the critical importance of avoiding overlaps with obstacles. When $d_i^t \geq R_c$, the penalty is zero, indicating a safe distance. This exponential design ensures heightened sensitivity near obstacles, particularly in dynamic or high-risk scenarios.

The DAC penalty is defined as:

$$\varphi_{\text{dac}}(d_i^t) = \max(0, R_c - d_i^t), \tag{8}$$

which increases linearly as d_i^t approaches the boundary ($d_i^t < R_c$). This formulation encourages smooth corrective actions and avoids over-penalizing minor deviations. For $d_i^t \geq R_c$, the penalty is zero, indicating compliance.

Training Objective. The $E_k(\tau)$ is transformed into a soft binary indicator by comparing it to a threshold ϵ. The module predicts this signal using a likelihood prediction head, which outputs the logits $f_k(\tau)$. These logits are optimized using the Binary Cross-Entropy Loss with Logits, defined as:

$$\mathcal{L}_c = \sum_{k \in \{\text{nfc},\text{dac}\}} \text{BCEWithLogits}(f_k(\tau), \mathbb{I}[E_k(\tau) > \epsilon]), \tag{9}$$

where $\mathbb{I}[E_k(\tau) > \epsilon]$ is the threshold indicator for each safety objective ($k \in \{\text{nfc}, \text{dac}\}$), and $E_k(\tau)$ is the Violation Energy Score associated with the respective constraint. The total loss function combines the constraint loss $\mathcal{L}_c$ with an imitation loss $\mathcal{L}_{\text{imitation}}$, which predicts the imitation error of the driven trajectory. The total loss is given by:

$$\mathcal{L}_{\text{total}} = \mathcal{L}_{\text{imitation}} + \mathcal{L}_c = \|\mathbf{e} - \hat{\mathbf{e}}\|^2 + \mathcal{L}_c, \tag{10}$$

where $\mathbf{e}$ is the ground-truth imitation error, and $\hat{\mathbf{e}}$ is the predicted imitation error. During inference, the module predicts $\hat{E}_{nfc} = \sigma(f_{\text{nfc}}(\tau))$, the estimated probability of a collision violation, and $\hat{E}_{dac} = \sigma(f_{\text{dac}}(\tau))$, the estimated probability of a drivable area compliance violation. Additionally, the predicted imitation error $\hat{\mathbf{e}}$ is output to estimate trajectory imitation performance.

3.4 Ensemble with Trajectory Probability

As mentioned in Section 3.1, motion planning generates N_m candidate trajectories $Y_0^{1:T_f} = \{(y_{0,i}^{1:T_f}, p_i)\}_{i=1}^{N_m}$, where p_i denotes the probability of the i-th candidate trajectory. The final trajectory τ^* is selected by maximizing p_i, subject to traffic and safety constraints. To align with the planner's decision-making, we combine the module-predicted score with trajectory probabilities. Instead of directly using softmax probabilities, according to [20], we adopt an energy-based score E_p to reflect the planner's confidence in its planned trajectory τ^*. The InD score quantifies a scenario's similarity with the training distribution and is defined as:

$$E_p = \log \sum_{i=1}^{N_m} \exp(p_i), \quad E_{InD} = \lambda \log p_1(\mathbf{z}_1) + (1-\lambda) E_p, \tag{11}$$

where $\log p_1(\mathbf{z}_1)$ represents the normalized log-likelihood of the scene context from Flow Matching. A high E_p indicates the planner is confident in its distribution of candidate trajectories.

For decision uncertainty estimation,

$$E_{nfc} = \lambda \hat{E}_{nfc} + (1-\lambda) E_p, \quad E_{dac} = \lambda \hat{E}_{dac} + (1-\lambda) E_p, \tag{12}$$

where $\hat{E}_{nfc}$ and $\hat{E}_{dac}$ are the predicted collision and compliance risks. Normalization ensures that all risk terms and E_p are on a comparable scale. The hyperparameter $\lambda \in [0, 1]$ controls the relative weighting of the predicted violation risks versus the trajectory's confidence.

4 Experiments

We first outline our experimental settings. Next, we present the quantitative results for the OOD Detection module and the Decision Uncertainty Estimation module, respectively, followed by ablation studies. These results demonstrate that each module significantly outperforms existing methods, offering more reliable safety validation. Finally, we provide qualitative demonstrations showing that the duo validation approach REDOUBT, based on these two modules, effectively categorizes driving situations into four types. Notably, it uncovers two unsafe situations overlooked by existing works, achieving more comprehensive safety guarantees for autonomous vehicles.

4.1 Experimental Setups

Dataset. We conduct our evaluations using nuPlan [4], which is currently the most widely used and the only large-scale dataset for motion planning evaluation. This dataset has 73 unique and well-labeled scenario types, defined by low-level driving attributes. We partition the dataset based on scenario frequency, following a strategy similar to that used in Shifts [36]. Specifically, the top 50% most frequent scenario types—which account for 95% of the total data—are categorized as the In-Distribution (InD) set, while the remaining, less common scenarios constitute the Out-of-Distribution (OOD) set. For more details, please refer to Appendix A.1

Our evaluations are carried out across three planning evaluation modes defined by the nuPlan [4]: (1) **Open-loop (OP):** The evaluation is conducted using log replay. *Notably, open-loop tests have limited value for motion planning, which continuously interacts with environments. However, they remain relevant in scenarios with mainly static obstacles, so we include them for evaluation completeness.* (2) **Closed-loop Non-Reactive (CNR):** Both the ego vehicle and other agents can deviate from their original trajectories, but the agents are non-reactive. (3) **Closed-loop Reactive (CR):** Both the ego vehicle and other agents can deviate, and the agents are reactive to the ego vehicle's behavior.

Planners. Our REDOUBT framework can be universally applied to various motion planning solutions to validate the safety of their planning results. To evaluate its effectiveness and model-agnostic nature, we integrate REDOUBT into the latent spaces of four diverse learning-based motion planners introduced in Related Work 2: **PlanTF**, **PLUTO**, **GameFormer**, and **PlanScope**. For implementation details, please refer to Appendix A.2.

Baselines. REDOUBT is evaluated on: (1) OOD Detection and (2) Decision Uncertainty Estimation. For OOD Detection, we compare against post hoc methods (MSP [19], MaxLogit [18], Entropy [35], Energy [34]) and feature-space methods (Mahalanobis Distance (MDS) [26], KNN [40], lGMM [44]).

For decision uncertainty estimation, we evaluate in Closed-loop (CNR and CR) and Open-loop (OP) settings. Closed-loop metrics include (1) No At-Fault Collisions (NFC), assessing whether the ego vehicle avoids fault-based collisions, and (2) Drivable Area Compliance (DAC), checking trajectory adherence to drivable areas. In the OP setting, we compute Average Displacement Error (ADE) within a bounded region. NFC and DAC are compared with the Energy score method, while ADE is evaluated against Shifts [36] baselines: Model Averaging (MA) and VAR [13].

Evaluation Metrics. We evaluate OOD detection using: (1) the false positive rate (FPR95) of OOD samples when the true positive rate of InD samples is 95%, and (2) the area under the receiver operating characteristic curve (AUROC). For decision uncertainty estimation, we consider: (1) the false positive rate (FPR95) of (No At-Fault Collision)/(Driving Area Compliance) samples when the true positive rate of violation samples is 95%, and (2) the AUROC. For imitation error, we use the area under the error-retention curve (R-AUC), which tracks trajectory imitation error as ground-truth labels progressively replace predictions in descending order of predicted error.

4.2 Evaluation of OOD Detection

Our method consistently outperforms existing OOD detection approaches across all three evaluation modes. As shown in Table 1, which compares OOD detection methods trained with the same four motion planning models, our approach achieves notable improvements in both FPR95 reduction and AUROC increase in OP, CNR, and CR modes. These advancements stem from the effective density estimation of InD features. Moreover, our method demonstrates strong performance across various motion planners, highlighting its versatility and reliability under diverse evaluation conditions.

Table 1: Comparison with OOD detection methods trained with the four motion planning models across three evaluation modes on nuPlan dataset. ↑ indicates larger values are better and vice versa. The best result in each column is shown in **bolded**. OP: Open-loop evaluation mode. CNR: Closed-loop non-reactive evaluation mode. CR: Closed-loop reactive evaluation mode.

Mode	**Method**	**PlanTF**		**PLUTO**		**GameFormer**		**PlanScope**		**Average**	
		FPR95 ↓	AUROC ↑	FPR95 ↓	AUROC ↑	FPR95 ↓	AUROC ↑	FPR95 ↓	AUROC ↑	FPR95 ↓	AUROC ↑
OP	MSP	88.92	64.29	79.70	74.15	91.16	62.13	83.85	71.37	85.91	67.99
	MaxLogit	69.04	75.14	64.99	74.06	93.84	54.08	83.86	71.65	77.93	68.73
	Entropy	88.96	58.77	71.56	62.64	96.77	50.89	84.24	66.87	85.38	59.79
	Energy	67.77	75.93	65.17	76.50	87.43	55.56	73.74	74.17	73.53	70.54
	MDS	94.54	65.81	69.02	80.55	70.05	70.43	81.32	76.74	78.73	73.38
	KNN	89.31	66.87	71.05	79.03	62.66	80.24	84.44	76.70	76.87	75.71
	lGMM	94.54	65.81	66.30	79.51	87.28	70.72	72.38	79.87	80.13	73.98
	REDOUBT(Ours)	**51.02**	**84.48**	**53.54**	**85.50**	**59.59**	**84.82**	**56.18**	**85.83**	**55.08**	**85.16**
CNR	MSP	91.22	59.50	80.94	73.56	91.60	59.65	84.23	70.68	87.00	65.85
	MaxLogit	77.79	69.68	66.84	78.24	92.81	52.71	76.53	74.61	78.49	68.81
	Entropy	92.21	55.83	75.17	62.79	95.96	51.39	82.07	65.65	86.35	58.91
	Energy	76.75	70.19	65.44	76.55	92.81	52.72	74.64	74.41	77.41	68.47
	MDS	92.39	65.45	63.49	81.50	68.74	71.68	69.39	80.09	73.50	74.68
	KNN	90.56	66.05	74.99	78.46	**65.80**	77.58	75.85	78.10	76.80	75.05
	lGMM	88.77	67.10	76.51	77.83	68.88	77.26	67.89	79.93	75.51	75.53
	REDOUBT(Ours)	**65.11**	**81.41**	**57.11**	**84.83**	66.35	**80.22**	**50.10**	**85.54**	**59.67**	**83.00**
CR	MSP	88.03	58.26	84.19	69.20	94.94	51.94	85.99	65.52	88.29	61.23
	MaxLogit	81.79	64.98	71.93	72.83	91.77	58.47	74.96	70.67	80.11	66.74
	Entropy	93.29	51.17	75.17	62.79	94.00	53.35	83.11	65.27	86.39	58.15
	Energy	81.25	65.36	71.38	70.36	93.84	54.08	73.25	71.25	79.93	65.26
	MDS	90.84	69.52	68.13	79.83	68.81	71.47	70.81	73.71	74.65	73.63
	KNN	90.01	66.14	73.23	78.66	67.17	77.01	67.00	80.82	74.35	75.66
	lGMM	86.31	71.74	74.41	77.37	69.33	76.63	73.34	76.96	75.85	75.68
	REDOUBT(Ours)	**61.81**	**81.81**	**59.14**	**82.58**	**66.83**	**80.32**	**58.12**	**83.47**	**61.48**	**82.05**

Figure 2: Retention curves of uncertainty estimation in open-loop evaluation across different planners. The ADE is plotted over the retention fraction. Lower R-AUC values indicate better performance. The oracle retention curve (green) is obtained by sorting samples in descending order of true ADE.

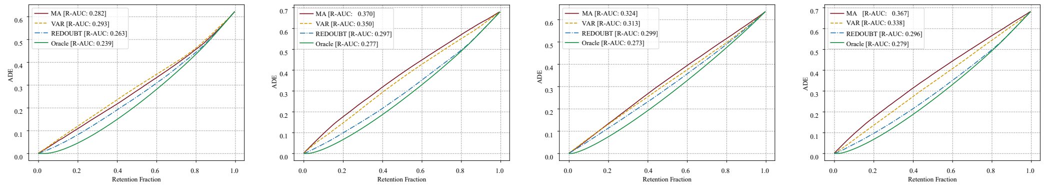

(a) PlanTF (b) PLUTO (c) GameFormer (d) PlanScope

4.3 Evaluation of Decision Uncertainty Estimation

Closed-loop Evaluation. Table 2 presents the evaluation results of uncertainty estimation, including No At-fault Collision (NFC) and Driving Area Compliance (DAC) under the closed-loop non-reactive and closed-loop reactive modes. Our method demonstrates superior performance across all four motion planners. For example, for predicting NFC violations, our method improves the average AUROC by 12.81% and 10.03% in the CNR mode and the CR mode, respectively.

Table 2: Comparison of NFC and DAC estimation results, trained with the four motion planning models and evaluated under the CNR and CR modes on nuPlan dataset.

Mode	**Uncertainty**	**Method**	**PlanTF**		**PLUTO**		**GameFormer**		**PlanScope**		**Average**	
			FPR95 ↓	AUROC ↑	FPR95 ↓	AUROC ↑	FPR95 ↓	AUROC ↑	FPR95 ↓	AUROC ↑	FPR95 ↓	AUROC ↑
CNR	NFC	Energy	79.33	63.10	89.52	66.36	91.63	52.93	73.40	57.30	83.47	59.92
		REDOUBT(Ours)	**70.93**	**70.45**	**68.04**	**71.62**	**56.85**	**74.44**	**57.30**	**74.41**	**63.28**	**72.73**
	DAC	Energy	76.88	59.01	76.70	63.31	95.38	51.19	69.36	66.21	79.58	59.93
		REDOUBT(Ours)	**55.13**	**82.33**	**52.97**	**77.33**	**52.36**	**75.38**	**55.94**	**75.00**	**54.10**	**77.51**
CR	NFC	Energy	82.74	64.39	82.27	71.58	87.88	59.62	80.84	67.24	83.43	65.71
		REDOUBT(Ours)	**67.04**	**71.97**	**58.29**	**78.11**	**57.34**	**73.37**	**49.22**	**79.51**	**57.97**	**75.74**
	DAC	Energy	66.98	70.88	80.26	55.73	80.53	67.95	69.67	73.70	74.36	67.07
		REDOUBT(Ours)	**52.24**	**84.03**	**58.59**	**76.90**	**51.63**	**76.90**	**48.67**	**80.00**	**52.78**	**79.46**

Open-loop Evaluation. The retention curves of uncertainty estimation under the open-loop evaluation mode, as shown in Figure 2, demonstrate that our method consistently performs closer to the Oracle retention compared to the best baselines across multiple planners. For example, in the PlanTF planner, our method achieves an ADE R-AUC of 0.263, which is closer to the Oracle value of 0.239, compared to the best baseline (0.282). This indicates that our method exhibits better uncertainty calibration, as it effectively aligns uncertainty estimates with the true ADE.

4.4 Evaluation of Duo Safety Validation

We evaluate the full REDOUBT system under a closed-loop reactive setting, jointly using OOD detection and decision uncertainty estimation. We report recall as the primary metric, measuring coverage of potential unsafe scenarios. Here, potential unsafe scenarios comprise three categories: InD + Uncertain (InD inputs with driving violations), OOD + Uncertain (OOD inputs with driving violations), and OOD + Certain (OOD inputs without driving violations). Further qualitative analysis of unsafe scenarios is provided in Section 4.6.

Table 3: Duo safety validation under closed-loop reactive mode: recall across OOD detection and decision uncertainty estimation

Method	PlanTF	PLUTO	GameFormer	PlanScope	Avg.
lGMM	53.50	65.88	51.81	49.95	55.29
Energy	59.52	65.82	64.97	72.61	65.73
REDOUBT	**90.24**	**90.52**	**91.34**	**90.02**	**90.53**
Category	**Decomposition of Recall by Scenario Category**				
InD+Uncertain	0.70	1.26	1.79	0.87	1.16
OOD+Certain	10.04	15.61	10.50	6.78	10.73
OOD+Uncertain	79.50	73.65	79.05	82.37	78.64

REDOUBT attains 90.53% recall, substantially outperforming strong baselines—55.29% for driving uncertainty estimation and 65.73% for OOD detection alone. This indicates that the unified design captures a broader set of unsafe cases.

We further decompose recall by category. OOD + Uncertain constitutes the majority (78.64%). InD + Uncertain accounts for 1.16%; despite its small share, these cases are safety critical. OOD + Certain contributes an additional 10.73%, reflecting OOD situations that may not immediately cause violations but remain hazardous under distribution shift. These results underscore the value of unifying OOD detection with decision uncertainty estimation for safety validation.

4.5 Ablation Studies

We conduct ablation experiments to evaluate the importance of the component design in our method.

Impact of Trajectory Probability Energy. We analyze the impact of incorporating the trajectory probability energy (E_p) on OOD detection and NFC and DAC estimation. Table 4 summarizes the average evaluation results without (w/o) and with E_p (REDOUBT). Notably, the inclusion of E_p significantly enhances OOD detection under all modes and NFC and DAC estimation under the CNR and CR modes. These findings demonstrate E_p's effectiveness in improving OOD detection and uncertainty estimation, as it is enhanced by encoding trajectory probability information. Additionally, we analyze the sensitivity of the ensemble weight λ, which balances the contributions of flow matching and E_p in Appendix B.4.

Table 4: Effects of Trajectory Probability Energy E_p on OOD detection and Uncertainty Estimation.

Metric	Method	OOD			NFC		DAC	
		OP	**CNR**	**CR**	**CNR**	**CR**	**CNR**	**CR**
FPR95 ↓	**w/o** E_p	62.08	71.06	63.47	71.85	69.42	62.86	56.15
	w/E_p	**55.08**	**59.67**	**61.48**	**63.28**	**57.97**	**54.10**	**52.78**
AUROC ↑	**w/o** E_p	83.23	78.47	80.82	68.18	72.12	77.02	78.58
	w/E_p	**85.16**	**83.00**	**82.05**	**72.73**	**75.74**	**77.51**	**79.46**

Impact of Gaussian Fourier Projection. Table 5 demonstrates the impact of the Gaussian Fourier Projection (GFP) on OOD detection performance across three modes (OP, CNR, and CR). GFP, which embeds the scalar time t into a high-dimensional feature vector, consistently improves AUROC scores. These results prove the effectiveness of GFP in capturing temporal features for better OOD detection. Further details are provided in Appendix B.2.

Table 5: Effects of GFP module and GMM Prior.

Mode	Module	FPR95 ↓	AUROC ↑
OP	w/o GFP	61.67	82.88
	w/o GMM	61.11	84.42
	REDOUBT	**55.08**	**85.16**
CNR	w/o GFP	62.67	82.15
	w/o GMM	61.68	82.79
	REDOUBT	**59.67**	**83.00**
CR	w/o GFP	63.68	80.87
	w/o GMM	70.33	75.46
	REDOUBT	**61.48**	**82.05**

Impact of Gaussian Mixture Model Prior. The ablation study in Table 5 examines the impact of using a Gaussian Mixture Model (GMM) prior in flow matching, compared to a Standard Normal distribution. The results consistently demonstrate that the GMM prior enhances Out-of-Distribution (OOD) detection performance across all modes. Further details are provided in Appendix B.3.

4.6 Demonstration of Duo Safety Validation

REDOUBT simultaneously inspects input distributions and output uncertainty, categorizing driving situations into four combinations based on the interplay of InD/OOD scenarios and certain/uncertain planning decisions. See Figure 3 for examples of each category.

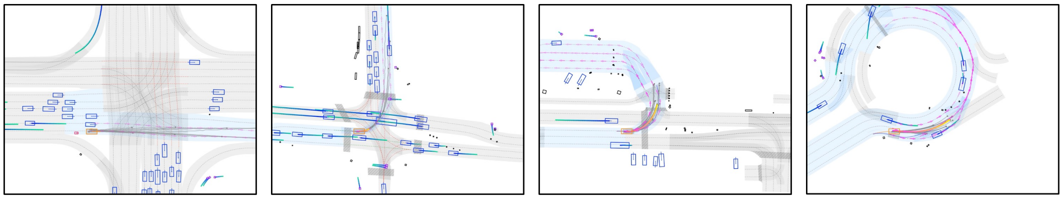

(a) InD + Certain (Safe)

(b) InD + Uncertain (Unsafe)

(c) OOD + Certain (Unsafe)

(d) OOD + Uncertain (Unsafe)

Figure 3: Safety categorization in REDOUBT: (a) **InD + Certain** (Safe, e.g., straight intersection traversal); (b) **InD + Uncertain** (Unsafe, e.g., high-density left turns with trained-but-failed scenarios); (c) **OOD + Certain** (Unsafe, e.g., overconfident unprotected cross-turns); (d) **OOD + Uncertain** (Unsafe, e.g., exiting drivable areas at drop-off locations). The scenarios illustrated include: Orange lines for the planned trajectory of the motion planner, Blue lines for the predicted trajectories of agents, and Gray lines for the candidate trajectories by the planner.

REDOUBT identifies two previously overlooked unsafe modes and illustrates them with representative failures. First, the InD + Uncertain scenario is overlooked by an input-only inspection that treats all InD as safe. Even in familiar scenarios, inherent complexity can induce uncertain decisions and unsafe outcomes. In Case (b), the High-Density Traffic during Left Turns scenario involves a left-turn maneuver in a high-density traffic environment, which is a common challenge for motion planners. Although this category of scenario was encountered during training, we observed that the planned trajectory by PlanScope planner and the candidate trajectories still resulted in a collision with surrounding vehicles. This failure highlights the complexity of high-density interactions where subtle variations can lead to collisions despite prior training exposure.

Second, the OOD + Certain scenario is overlooked by output-only inspection that treats all "certain" decisions as safe. Rare scenarios can induce overconfident decisions that remain hazardous under shift. In Case (c), the Unprotected Cross-Turns scenario involves unprotected cross-turns, a category of scene that was not observed during training. Despite the absence of such scenarios in the training data, the planner still needs to output decisions. In Case (d), the Traversing Pickup/Drop-Off Areas scenario involves the ego vehicle traversing a drop-off area while not stopping. Such scenarios were also not present in the training data, and we observed that the planned trajectory drifted outside the drivable area. This failure illustrates the planner's limitations in handling complex, context-specific scenarios that require precise spatial reasoning and awareness.

5 Conclusion

In this work, we propose REDOUBT, a duo safety validation framework for autonomous vehicle motion planning that addresses two critical aspects: OOD detection and decision uncertainty estimation. Our approach introduces a latent flow matching method to model distributional shifts and detect OOD traffic scenarios, effectively capturing the planning contexts' multi-modal and dynamic nature. Additionally, we design an energy-based risk prediction method that integrates trajectory probabilities and risk signals to estimate decision uncertainty without relying on explicit violation labels. Experiments and ablation studies on the nuPlan dataset validate the effectiveness and versatility of REDOUBT, demonstrating its ability to identify previously overlooked unsafe situations.

Acknowledgement

The work is supported in part by Hong Kong Research Grant Council under CRF C1042-23GF and GRF 11216323.

References

[1] Pasquale Antonante, Sushant Veer, Karen Leung, Xinshuo Weng, Luca Carlone, and Marco Pavone. Task-aware risk estimation of perception failures for autonomous vehicles. *arXiv preprint arXiv:2305.01870*, 2023.

[2] Heli Ben-Hamu, Samuel Cohen, Joey Bose, Brandon Amos, Aditya Grover, Maximilian Nickel, Ricky TQ Chen, and Yaron Lipman. Matching normalizing flows and probability paths on manifolds. *arXiv preprint arXiv:2207.04711*, 2022.

[3] Julian Bitterwolf, Maximilian Mueller, and Matthias Hein. In or out? fixing imagenet out-of-distribution detection evaluation. In *ICML*, 2023.

[4] Holger Caesar, Juraj Kabzan, Kok Seang Tan, Whye Kit Fong, Eric Wolff, Alex Lang, Luke Fletcher, Oscar Beijbom, and Sammy Omari. nuplan: A closed-loop ml-based planning benchmark for autonomous vehicles. *arXiv preprint arXiv:2106.11810*, 2021.

[5] Li Chen, Penghao Wu, Kashyap Chitta, Bernhard Jaeger, Andreas Geiger, and Hongyang Li. End-to-end autonomous driving: Challenges and frontiers. *IEEE Transactions on Pattern Analysis and Machine Intelligence*, 2024.

[6] Ricky TQ Chen, Yulia Rubanova, Jesse Bettencourt, and David K Duvenaud. Neural ordinary differential equations. *Advances in neural information processing systems*, 31, 2018.

[7] Jie Cheng, Yingbing Chen, and Qifeng Chen. Pluto: Pushing the limit of imitation learning-based planning for autonomous driving. *arXiv preprint arXiv:2404.14327*, 2024.

[8] Jie Cheng, Yingbing Chen, Xiaodong Mei, Bowen Yang, Bo Li, and Ming Liu. Rethinking imitation-based planner for autonomous driving, 2023.

[9] Quan Dao, Hao Phung, Binh Nguyen, and Anh Tran. Flow matching in latent space. *arXiv preprint arXiv:2307.08698*, 2023.

[10] Daniel Dauner, Marcel Hallgarten, Andreas Geiger, and Kashyap Chitta. Parting with misconceptions about learning-based vehicle motion planning. In *Conference on Robot Learning (CoRL)*, 2023.

[11] Christopher Diehl, Peter Karkus, Sushant Veer, Marco Pavone, and Torsten Bertram. Lord: Adapting differentiable driving policies to distribution shifts. In *International Conference on Robotics and Automation*, 2025.

[12] Coco Feng. Xiaomi founder has ‘the hardest time’ since fatal crash involving one of its cars. *South China Morning Post*, 2025. Published: May 10, 2025.

[13] Angelos Filos, Panagiotis Tigas, Rowan McAllister, Nicholas Rhinehart, Sergey Levine, and Yarin Gal. Can autonomous vehicles identify, recover from, and adapt to distribution shifts? In *International Conference on Machine Learning (ICML)*, 2020.

[14] Tor Fjelde, Emile Mathieu, and Vincent Dutordoir. An introduction to flow matching, January 2024.

[15] Soumya Suvra Ghosal, Yiyou Sun, and Yixuan Li. How to overcome curse-of-dimensionality for out-of-distribution detection? In *Proceedings of the AAAI Conference on Artificial Intelligence*, volume 38, pages 19849–19857, 2024.

[16] Xunjiang Gu, Guanyu Song, Igor Gilitschenski, Marco Pavone, and Boris Ivanovic. Producing and leveraging online map uncertainty in trajectory prediction. In *Proceedings of the IEEE/CVF Conference on Computer Vision and Pattern Recognition (CVPR)*, pages 14521–14530, June 2024.

[17] K. Tan et al. H. Caesar, J. Kabzan. Nuplan: A closed-loop ml-based planning benchmark for autonomous vehicles. In *CVPR ADP3 workshop*, 2021.

[18] Dan Hendrycks, Steven Basart, Mantas Mazeika, Andy Zou, Joe Kwon, Mohammadreza Mostajabi, Jacob Steinhardt, and Dawn Song. Scaling out-of-distribution detection for real-world settings. *arXiv preprint arXiv:1911.11132*, 2019.

[19] Dan Hendrycks and Kevin Gimpel. A baseline for detecting misclassified and out-of-distribution examples in neural networks. *Proceedings of International Conference on Learning Representations*, 2017.

[20] Claus Hofmann, Simon Schmid, Bernhard Lehner, Daniel Klotz, and Sepp Hochreiter. Energy-based hopfield boosting for out-of-distribution detection. *arXiv preprint arXiv:2405.08766*, 2024.

[21] Hong Huang and Dapeng Wu. Quaff: Quantized parameter-efficient fine-tuning under outlier spatial stability hypothesis, 2025.

[22] Zhiyu Huang, Haochen Liu, and Chen Lv. Gameformer: Game-theoretic modeling and learning of transformer-based interactive prediction and planning for autonomous driving. In *Proceedings of the IEEE/CVF International Conference on Computer Vision (ICCV)*, pages 3903–3913, October 2023.

[23] Xiaosong Jia, Penghao Wu, Li Chen, Yu Liu, Hongyang Li, and Junchi Yan. Hdgt: Heterogeneous driving graph transformer for multi-agent trajectory prediction via scene encoding. *IEEE transactions on pattern analysis and machine intelligence*, 45(11):13860–13875, 2023.

[24] Bo Jiang, Shaoyu Chen, Qing Xu, Bencheng Liao, Jiajie Chen, Helong Zhou, Qian Zhang, Wenyu Liu, Chang Huang, and Xinggang Wang. Vad: Vectorized scene representation for efficient autonomous driving. In *Proceedings of the IEEE/CVF International Conference on Computer Vision*, pages 8340–8350, 2023.

[25] Zhiqian Lan, Yuxuan Jiang, Yao Mu, Chen Chen, and Shengbo Eben Li. Sept: Towards efficient scene representation learning for motion prediction. *arXiv preprint arXiv:2309.15289*, 2023.

[26] Kimin Lee, Kibok Lee, Honglak Lee, and Jinwoo Shin. A simple unified framework for detecting out-of-distribution samples and adversarial attacks. *Advances in neural information processing systems*, 31, 2018.

[27] Boqi Li, Haojie Zhu, and Henry X. Liu. Decode: Domain-aware continual domain expansion for motion prediction, 2024.

[28] Quanyi Li, Zhenghao Peng, Lan Feng, Zhizheng Liu, Chenda Duan, Wenjie Mo, and Bolei Zhou. Scenarionet: Open-source platform for large-scale traffic scenario simulation and modeling. *Advances in Neural Information Processing Systems*, 2023.

[29] Yiming Li, Zehong Wang, Yue Wang, Zhiding Yu, Zan Gojcic, Marco Pavone, Chen Feng, and Jose M. Alvarez. Memorize what matters: Emergent scene decomposition from multitraverse. In *Advances in Neural Information Processing Systems (NeurIPS)*, 2024.

[30] Yaron Lipman, Ricky TQ Chen, Heli Ben-Hamu, Maximilian Nickel, and Matt Le. Flow matching for generative modeling. *arXiv preprint arXiv:2210.02747*, 2022.

[31] Yaron Lipman, Marton Havasi, Peter Holderrieth, Neta Shaul, Matt Le, Brian Karrer, Ricky TQ Chen, David Lopez-Paz, Heli Ben-Hamu, and Itai Gat. Flow matching guide and code. *arXiv preprint arXiv:2412.06264*, 2024.

[32] Litian Liu and Yao Qin. Fast decision boundary based out-of-distribution detector. *ICML*, 2024.

[33] Mengmeng Liu, Hao Cheng, Lin Chen, Hellward Broszio, Jiangtao Li, Runjiang Zhao, Monika Sester, and Michael Ying Yang. Laformer: Trajectory prediction for autonomous driving with lane-aware scene constraints. In *Proceedings of the IEEE/CVF Conference on Computer Vision and Pattern Recognition*, pages 2039–2049, 2024.

[34] Weitang Liu, Xiaoyun Wang, John Owens, and Yixuan Li. Energy-based out-of-distribution detection. *Advances in Neural Information Processing Systems*, 2020.

[35] Juanwu Lu, Can Cui, Yunsheng Ma, Aniket Bera, and Ziran Wang. Quantifying uncertainty in motion prediction with variational bayesian mixture. In *Proceedings of the IEEE/CVF Conference on Computer Vision and Pattern Recognition (CVPR)*, pages 15428–15437, June 2024.

[36] Andrey Malinin, Neil Band, Alexander Ganshin, German Chesnokov, Yarin Gal, Mark J. F. Gales, Alexey Noskov, Andrey Ploskonosov, Liudmila Prokhorenkova, Ivan Provilkov, Vatsal Raina, Vyas Raina, Denis Roginskiy, Mariya Shmatova, Panos Tigar, and Boris Yangel. Shifts: A dataset of real distributional shift across multiple large-scale tasks. *arXiv preprint arXiv:2107.07455*, 2021.

[37] Jianbiao Mei, Yukai Ma, Xuemeng Yang, Licheng Wen, Xinyu Cai, Xin Li, Daocheng Fu, Bo Zhang, Pinlong Cai, Min Dou, et al. Continuously learning, adapting, and improving: A dual-process approach to autonomous driving. *arXiv preprint arXiv:2405.15324*, 2024.

[38] Liang Peng, Boqi Li, Wenhao Yu, Kai Yang, Wenbo Shao, and Hong Wang. Sotif entropy: Online sotif risk quantification and mitigation for autonomous driving. *IEEE Transactions on Intelligent Transportation Systems*, 25(2):1530–1546, 2024.

[39] Shaoshuai Shi, Li Jiang, Dengxin Dai, and Bernt Schiele. Motion transformer with global intention localization and local movement refinement. *Advances in Neural Information Processing Systems*, 2022.

[40] Yiyou Sun, Yifei Ming, Xiaojin Zhu, and Yixuan Li. Out-of-distribution detection with deep nearest neighbors. *ICML*, 2022.

[41] Eli Verwimp, Kuo Yang, Sarah Parisot, Lanqing Hong, Steven McDonagh, Eduardo Pérez-Pellitero, Matthias De Lange, and Tinne Tuytelaars. Clad: A realistic continual learning benchmark for autonomous driving. *Neural Networks*, 161:659–669, 2023.

[42] Yun Wang, Junjie Hu, Junhui Hou, Chenghao Zhang, Renwei Yang, and Dapeng Oliver Wu. Rose: Robust self-supervised stereo matching under adverse weather conditions. *arXiv preprint arXiv:2509.19165*, 2025.

[43] Yun Wang, Jiahao Zheng, Chenghao Zhang, Zhanjie Zhang, Kunhong Li, Yongjian Zhang, and Junjie Hu. Dualnet: Robust self-supervised stereo matching with pseudo-label supervision. In *Proceedings of the AAAI Conference on Artificial Intelligence*, volume 39, pages 8178–8186, 2025.

[44] Julian Wiederer, Julian Schmidt, Ulrich Kressel, Klaus Dietmayer, and Vasileios Belagiannis. Joint out-of-distribution detection and uncertainty estimation for trajectory prediction. In *2023 IEEE/RSJ International Conference on Intelligent Robots and Systems (IROS)*, pages 5487–5494. IEEE, 2023.

[45] Wei Wu, Xiaoxin Feng, Ziyan Gao, and Yuheng Kan. Smart: Scalable multi-agent real-time simulation via next-token prediction. *arXiv preprint arXiv:2405.15677*, 2024.

[46] Ren Xin, Jie Cheng, and Jun Ma. PlanScope: learning to plan within decision scope does matter, 2024.

[47] Ren Xin, Hongji Liu, Yingbing Chen, Jie Cheng, Sheng Wang, Jun Ma, and Ming Liu. A generic trajectory planning method for constrained all-wheel-steering robots. In *Proceedings of the IEEE/RSJ International Conference on Intelligent Robots and Systems*, 2024.

[48] Zebin Xing, Xingyu Zhang, Yang Hu, Bo Jiang, Tong He, Qian Zhang, Xiaoxiao Long, and Wei Yin. Goalflow: Goal-driven flow matching for multimodal trajectories generation in end-to-end autonomous driving. *arXiv preprint arXiv:2503.05689*, 2025.

[49] Jingkang Yang, Kaiyang Zhou, Yixuan Li, and Ziwei Liu. Generalized out-of-distribution detection: A survey. *arXiv preprint arXiv:2110.11334*, 2021.

[50] Boxuan Zhang, Jianing Zhu, Zengmao Wang, Tongliang Liu, Bo Du, and Bo Han. What if the input is expanded in ood detection? *Advances in Neural Information Processing Systems*, 37:21289–21329, 2024.

[51] Jingyang Zhang, Jingkang Yang, Pengyun Wang, Haoqi Wang, Yueqian Lin, Haoran Zhang, Yiyou Sun, Xuefeng Du, Yixuan Li, Ziwei Liu, Yiran Chen, and Hai Li. Openood v1.5: Enhanced benchmark for out-of-distribution detection. *arXiv preprint arXiv:2306.09301*, 2023.

[52] Junrui Zhang, Chenjie Wang, Jie Peng, Haoyu Li, Jianmin Ji, Yu Zhang, and Yanyong Zhang. Cafe-ad: Cross-scenario adaptive feature enhancement for trajectory planning in autonomous driving. *arXiv preprint arXiv:2504.06584*, 2025.

[53] Yonggang Zhang, Jie Lu, Bo Peng, Zhen Fang, and Yiu-ming Cheung. Learning to shape in-distribution feature space for out-of-distribution detection. In *The Thirty-eighth Annual Conference on Neural Information Processing Systems*, 2024.

[54] Yinan Zheng, Ruiming Liang, Kexin ZHENG, Jinliang Zheng, Liyuan Mao, Jianxiong Li, Weihao Gu, Rui Ai, Shengbo Eben Li, Xianyuan Zhan, and Jingjing Liu. Diffusion-based planning for autonomous driving with flexible guidance. In *The Thirteenth International Conference on Learning Representations*, 2025.

NeurIPS Paper Checklist

1. **Claims**

   Question: Do the main claims made in the abstract and introduction accurately reflect the paper's contributions and scope?

   Answer: [Yes]

   Justification: We have clearly stated the main contributions made in the paper and important assumptions and limitations in both the Abstract and the Introduction (Section 1).

   Guidelines:

   - The answer NA means that the abstract and introduction do not include the claims made in the paper.
   - The abstract and/or introduction should clearly state the claims made, including the contributions made in the paper and important assumptions and limitations. A No or NA answer to this question will not be perceived well by the reviewers.
   - The claims made should match theoretical and experimental results, and reflect how much the results can be expected to generalize to other settings.
   - It is fine to include aspirational goals as motivation as long as it is clear that these goals are not attained by the paper.

2. **Limitations**

   Question: Does the paper discuss the limitations of the work performed by the authors?

   Answer: [Yes]

   Justification: In Appendix Section D, we have discussed the limitations of this work.

   Guidelines:

   - The answer NA means that the paper has no limitation while the answer No means that the paper has limitations, but those are not discussed in the paper.
   - The authors are encouraged to create a separate "Limitations" section in their paper.
   - The paper should point out any strong assumptions and how robust the results are to violations of these assumptions (e.g., independence assumptions, noiseless settings, model well-specification, asymptotic approximations only holding locally). The authors should reflect on how these assumptions might be violated in practice and what the implications would be.
   - The authors should reflect on the scope of the claims made, e.g., if the approach was only tested on a few datasets or with a few runs. In general, empirical results often depend on implicit assumptions, which should be articulated.
   - The authors should reflect on the factors that influence the performance of the approach. For example, a facial recognition algorithm may perform poorly when image resolution is low or images are taken in low lighting. Or a speech-to-text system might not be used reliably to provide closed captions for online lectures because it fails to handle technical jargon.
   - The authors should discuss the computational efficiency of the proposed algorithms and how they scale with dataset size.
   - If applicable, the authors should discuss possible limitations of their approach to address problems of privacy and fairness.
   - While the authors might fear that complete honesty about limitations might be used by reviewers as grounds for rejection, a worse outcome might be that reviewers discover limitations that aren't acknowledged in the paper. The authors should use their best judgment and recognize that individual actions in favor of transparency play an important role in developing norms that preserve the integrity of the community. Reviewers will be specifically instructed to not penalize honesty concerning limitations.

3. **Theory assumptions and proofs**

   Question: For each theoretical result, does the paper provide the full set of assumptions and a complete (and correct) proof?

   Answer: [NA]

Justification: The paper does not include new theoretical results.

Guidelines:

- The answer NA means that the paper does not include theoretical results.
- All the theorems, formulas, and proofs in the paper should be numbered and cross-referenced.
- All assumptions should be clearly stated or referenced in the statement of any theorems.
- The proofs can either appear in the main paper or the supplemental material, but if they appear in the supplemental material, the authors are encouraged to provide a short proof sketch to provide intuition.
- Inversely, any informal proof provided in the core of the paper should be complemented by formal proofs provided in appendix or supplemental material.
- Theorems and Lemmas that the proof relies upon should be properly referenced.

4. **Experimental result reproducibility**

   Question: Does the paper fully disclose all the information needed to reproduce the main experimental results of the paper to the extent that it affects the main claims and/or conclusions of the paper (regardless of whether the code and data are provided or not)?

   Answer: [Yes]

   Justification: Yes, the paper discloses all the necessary details about the implemented architectures used, hyperparameters for each setting and other experimental details to reproduce all the experiments in the paper. These details can be found in Section A in the Appendix.

   Guidelines:

   - The answer NA means that the paper does not include experiments.
   - If the paper includes experiments, a No answer to this question will not be perceived well by the reviewers: Making the paper reproducible is important, regardless of whether the code and data are provided or not.
   - If the contribution is a dataset and/or model, the authors should describe the steps taken to make their results reproducible or verifiable.
   - Depending on the contribution, reproducibility can be accomplished in various ways. For example, if the contribution is a novel architecture, describing the architecture fully might suffice, or if the contribution is a specific model and empirical evaluation, it may be necessary to either make it possible for others to replicate the model with the same dataset, or provide access to the model. In general. releasing code and data is often one good way to accomplish this, but reproducibility can also be provided via detailed instructions for how to replicate the results, access to a hosted model (e.g., in the case of a large language model), releasing of a model checkpoint, or other means that are appropriate to the research performed.
   - While NeurIPS does not require releasing code, the conference does require all submissions to provide some reasonable avenue for reproducibility, which may depend on the nature of the contribution. For example
     (a) If the contribution is primarily a new algorithm, the paper should make it clear how to reproduce that algorithm.
     (b) If the contribution is primarily a new model architecture, the paper should describe the architecture clearly and fully.
     (c) If the contribution is a new model (e.g., a large language model), then there should either be a way to access this model for reproducing the results or a way to reproduce the model (e.g., with an open-source dataset or instructions for how to construct the dataset).
     (d) We recognize that reproducibility may be tricky in some cases, in which case authors are welcome to describe the particular way they provide for reproducibility. In the case of closed-source models, it may be that access to the model is limited in some way (e.g., to registered users), but it should be possible for other researchers to have some path to reproducing or verifying the results.

5. **Open access to data and code**

Question: Does the paper provide open access to the data and code, with sufficient instructions to faithfully reproduce the main experimental results, as described in supplemental material?

Answer: [No]

Justification: We will release the code upon acceptance of the paper.

Guidelines:

- The answer NA means that paper does not include experiments requiring code.
- Please see the NeurIPS code and data submission guidelines (`https://nips.cc/public/guides/CodeSubmissionPolicy`) for more details.
- While we encourage the release of code and data, we understand that this might not be possible, so "No" is an acceptable answer. Papers cannot be rejected simply for not including code, unless this is central to the contribution (e.g., for a new open-source benchmark).
- The instructions should contain the exact command and environment needed to run to reproduce the results. See the NeurIPS code and data submission guidelines (`https://nips.cc/public/guides/CodeSubmissionPolicy`) for more details.
- The authors should provide instructions on data access and preparation, including how to access the raw data, preprocessed data, intermediate data, and generated data, etc.
- The authors should provide scripts to reproduce all experimental results for the new proposed method and baselines. If only a subset of experiments are reproducible, they should state which ones are omitted from the script and why.
- At submission time, to preserve anonymity, the authors should release anonymized versions (if applicable).
- Providing as much information as possible in supplemental material (appended to the paper) is recommended, but including URLs to data and code is permitted.

6. **Experimental setting/details**

   Question: Does the paper specify all the training and test details (e.g., data splits, hyperparameters, how they were chosen, type of optimizer, etc.) necessary to understand the results?

   Answer: [Yes]

   Justification: In Section 4, we have briefly introduced the experimental setups about datasets, model setups, and evaluation metrics. Furthermore, we have provided full details of experimental settings in Appendix A.

   Guidelines:

   - The answer NA means that the paper does not include experiments.
   - The experimental setting should be presented in the core of the paper to a level of detail that is necessary to appreciate the results and make sense of them.
   - The full details can be provided either with the code, in appendix, or as supplemental material.

7. **Experiment statistical significance**

   Question: Does the paper report error bars suitably and correctly defined or other appropriate information about the statistical significance of the experiments?

   Answer: [Yes]

   Justification: In the ablation study to evaluate the significance of each component design in our method, and the factors of variability are clearly stated in Section 4.5. In Appendix B, we have provided the full results of this experiment.

   Guidelines:

   - The answer NA means that the paper does not include experiments.
   - The authors should answer "Yes" if the results are accompanied by error bars, confidence intervals, or statistical significance tests, at least for the experiments that support the main claims of the paper.

- The factors of variability that the error bars are capturing should be clearly stated (for example, train/test split, initialization, random drawing of some parameter, or overall run with given experimental conditions).
- The method for calculating the error bars should be explained (closed form formula, call to a library function, bootstrap, etc.)
- The assumptions made should be given (e.g., Normally distributed errors).
- It should be clear whether the error bar is the standard deviation or the standard error of the mean.
- It is OK to report 1-sigma error bars, but one should state it. The authors should preferably report a 2-sigma error bar than state that they have a 96% CI, if the hypothesis of Normality of errors is not verified.
- For asymmetric distributions, the authors should be careful not to show in tables or figures symmetric error bars that would yield results that are out of range (e.g. negative error rates).
- If error bars are reported in tables or plots, The authors should explain in the text how they were calculated and reference the corresponding figures or tables in the text.

8. **Experiments compute resources**

   Question: For each experiment, does the paper provide sufficient information on the computer resources (type of compute workers, memory, time of execution) needed to reproduce the experiments?

   Answer: [Yes]

   Justification:

   Guidelines: We have provided sufficient information on the computer resources, such as the type, amount, and memory of compute workers GPU required for the experiments in the reproducibility statement at the Appendix A.2.

   - The answer NA means that the paper does not include experiments.
   - The paper should indicate the type of compute workers CPU or GPU, internal cluster, or cloud provider, including relevant memory and storage.
   - The paper should provide the amount of compute required for each of the individual experimental runs as well as estimate the total compute.
   - The paper should disclose whether the full research project required more compute than the experiments reported in the paper (e.g., preliminary or failed experiments that didn't make it into the paper).

9. **Code of ethics**

   Question: Does the research conducted in the paper conform, in every respect, with the NeurIPS Code of Ethics `https://neurips.cc/public/EthicsGuidelines`?

   Answer: [Yes]

   Justification: The research conducted in the paper conforms, in every respect, with the NeurIPS Code of Ethics, and the authors remain anonymous.

   Guidelines:

   - The answer NA means that the authors have not reviewed the NeurIPS Code of Ethics.
   - If the authors answer No, they should explain the special circumstances that require a deviation from the Code of Ethics.
   - The authors should make sure to preserve anonymity (e.g., if there is a special consideration due to laws or regulations in their jurisdiction).

10. **Broader impacts**

    Question: Does the paper discuss both potential positive societal impacts and negative societal impacts of the work performed?

    Answer: [Yes]

    Justification: We have discussed the potential broader impact of this paper in Appendix E.

    Guidelines:

- The answer NA means that there is no societal impact of the work performed.
- If the authors answer NA or No, they should explain why their work has no societal impact or why the paper does not address societal impact.
- Examples of negative societal impacts include potential malicious or unintended uses (e.g., disinformation, generating fake profiles, surveillance), fairness considerations (e.g., deployment of technologies that could make decisions that unfairly impact specific groups), privacy considerations, and security considerations.
- The conference expects that many papers will be foundational research and not tied to particular applications, let alone deployments. However, if there is a direct path to any negative applications, the authors should point it out. For example, it is legitimate to point out that an improvement in the quality of generative models could be used to generate deepfakes for disinformation. On the other hand, it is not needed to point out that a generic algorithm for optimizing neural networks could enable people to train models that generate Deepfakes faster.
- The authors should consider possible harms that could arise when the technology is being used as intended and functioning correctly, harms that could arise when the technology is being used as intended but gives incorrect results, and harms following from (intentional or unintentional) misuse of the technology.
- If there are negative societal impacts, the authors could also discuss possible mitigation strategies (e.g., gated release of models, providing defenses in addition to attacks, mechanisms for monitoring misuse, mechanisms to monitor how a system learns from feedback over time, improving the efficiency and accessibility of ML).

11. **Safeguards**

    Question: Does the paper describe safeguards that have been put in place for responsible release of data or models that have a high risk for misuse (e.g., pretrained language models, image generators, or scraped datasets)?

    Answer: [NA]

    Justification: The paper poses no such risks.

    Guidelines:

    - The answer NA means that the paper poses no such risks.
    - Released models that have a high risk for misuse or dual-use should be released with necessary safeguards to allow for controlled use of the model, for example by requiring that users adhere to usage guidelines or restrictions to access the model or implementing safety filters.
    - Datasets that have been scraped from the Internet could pose safety risks. The authors should describe how they avoided releasing unsafe images.
    - We recognize that providing effective safeguards is challenging, and many papers do not require this, but we encourage authors to take this into account and make a best faith effort.

12. **Licenses for existing assets**

    Question: Are the creators or original owners of assets (e.g., code, data, models), used in the paper, properly credited and are the license and terms of use explicitly mentioned and properly respected?

    Answer: [Yes]

    Justification: All used assets in the paper are properly credited, and the datasets used in this paper are properly licensed.

    Guidelines:

    - The answer NA means that the paper does not use existing assets.
    - The authors should cite the original paper that produced the code package or dataset.
    - The authors should state which version of the asset is used and, if possible, include a URL.
    - The name of the license (e.g., CC-BY 4.0) should be included for each asset.

- For scraped data from a particular source (e.g., website), the copyright and terms of service of that source should be provided.
- If assets are released, the license, copyright information, and terms of use in the package should be provided. For popular datasets, `paperswithcode.com/datasets` has curated licenses for some datasets. Their licensing guide can help determine the license of a dataset.
- For existing datasets that are re-packaged, both the original license and the license of the derived asset (if it has changed) should be provided.
- If this information is not available online, the authors are encouraged to reach out to the asset's creators.

13. **New assets**

    Question: Are new assets introduced in the paper well documented and is the documentation provided alongside the assets?

    Answer: [NA]

    Justification: The paper does not release new assets.

    Guidelines:

    - The answer NA means that the paper does not release new assets.
    - Researchers should communicate the details of the dataset/code/model as part of their submissions via structured templates. This includes details about training, license, limitations, etc.
    - The paper should discuss whether and how consent was obtained from people whose asset is used.
    - At submission time, remember to anonymize your assets (if applicable). You can either create an anonymized URL or include an anonymized zip file.

14. **Crowdsourcing and research with human subjects**

    Question: For crowdsourcing experiments and research with human subjects, does the paper include the full text of instructions given to participants and screenshots, if applicable, as well as details about compensation (if any)?

    Answer: [NA]

    Justification: The paper does not involve crowdsourcing nor research with human subjects.

    Guidelines:

    - The answer NA means that the paper does not involve crowdsourcing nor research with human subjects.
    - Including this information in the supplemental material is fine, but if the main contribution of the paper involves human subjects, then as much detail as possible should be included in the main paper.
    - According to the NeurIPS Code of Ethics, workers involved in data collection, curation, or other labor should be paid at least the minimum wage in the country of the data collector.

15. **Institutional review board (IRB) approvals or equivalent for research with human subjects**

    Question: Does the paper describe potential risks incurred by study participants, whether such risks were disclosed to the subjects, and whether Institutional Review Board (IRB) approvals (or an equivalent approval/review based on the requirements of your country or institution) were obtained?

    Answer: [NA]

    Justification: The paper does not involve crowdsourcing nor research with human subjects.

    Guidelines:

    - The answer NA means that the paper does not involve crowdsourcing nor research with human subjects.

- Depending on the country in which research is conducted, IRB approval (or equivalent) may be required for any human subjects research. If you obtained IRB approval, you should clearly state this in the paper.
- We recognize that the procedures for this may vary significantly between institutions and locations, and we expect authors to adhere to the NeurIPS Code of Ethics and the guidelines for their institution.
- For initial submissions, do not include any information that would break anonymity (if applicable), such as the institution conducting the review.

16. **Declaration of LLM usage**

    Question: Does the paper describe the usage of LLMs if it is an important, original, or non-standard component of the core methods in this research? Note that if the LLM is used only for writing, editing, or formatting purposes and does not impact the core methodology, scientific rigorousness, or originality of the research, declaration is not required.

    Answer: [NA]

    Justification: This research does not involve LLMs as any important, original, or non-standard components.

    Guidelines:

    - The answer NA means that the core method development in this research does not involve LLMs as any important, original, or non-standard components.
    - Please refer to our LLM policy (`https://neurips.cc/Conferences/2025/LLM`) for what should or should not be described.

A More Experimental Details

A.1 Training Settings

The training dataset contains a total of 300,000 scenarios, including specific InD scenario types. The evaluation dataset consists of 19,685 scenarios, with fixed scenario tokens. For each scenario type (except for the "Unknown" scenario, which cannot be verified based on the scenario type), either 500 scenarios are included, or, if fewer than 500 scenarios are available, all the available scenarios are used. All planners are trained exclusively on the InD dataset and evaluated on the full dataset, which includes both InD and OOD scenarios.

A.2 Implementation Details

Motion Planning Model. Our experiments are conducted on a server with 8 NVIDIA RTX 5880 Ada GPUs and the Pytorch platform. The training experiments consist of two phases. In the first phase, each planner is trained according to its original settings. Specifically, PlanTF is trained with a batch size of 128, a weight decay of 1×10^{-4}, and for 25 epochs [8]. The learning rate starts at 1×10^{-3} and decays to zero following a cosine schedule. PLUTO is also trained with a batch size of 128 and a weight decay of 1×10^{-4} for 25 epochs [7]. Its learning rate is linearly increased to 1×10^{-3} over the first 3 epochs and then follows a cosine decay. GameFormer is trained with a batch size of 32, a weight decay of 0.01, and for 20 epochs [22]. The learning rate starts at 1×10^{-4} and halves every 2 epochs after the 10th epoch. PlanScope is trained with a batch size of 32 per GPU for 25 epochs, with 3 warm-up epochs, using the Adam optimizer and an initial learning rate of 1×10^{-3} [46].

REDOUBT Model. In the second phase, the flow matching and uncertainty prediction modules are optimized separately. The flow matching module is trained for 2000 epochs using the Adam optimizer, a batch size of 1024, and a cosine learning rate schedule with an initial learning rate of 1×10^{-3}. The uncertainty prediction module is trained for 25 epochs, also using the Adam optimizer, a batch size of 1024, and a fixed learning rate of 1×10^{-3}. During this phase, the weights of the scene encoder and trajectory prediction decoder are frozen to preserve motion planning performance.

B Additional Ablation Studies

Table 6: Detailed results of the ablation study on Trajectory Probability Energy E_p.

Evaluation	**Mode**	**Method**	**PlanTF**		**PLUTO**		**GameFormer**		**PlanScope**		**Average**	
			FPR95 ↓	AUROC ↑	FPR95 ↓	AUROC ↑	FPR95 ↓	AUROC ↑	FPR95 ↓	AUROC ↑	FPR95 ↓	AUROC ↑
OOD	OP	w/o E_p	62.20	82.19	62.60	82.30	62.93	83.67	60.60	84.74	62.08	83.23
		w/ E_p	**51.02**	**84.48**	**53.54**	**85.50**	**59.59**	**84.82**	**56.18**	**85.83**	**55.08**	**85.16**
	CNR	w/o E_p	90.48	69.10	65.35	81.52	66.83	79.92	61.58	83.32	71.06	78.47
		w/ E_p	**65.11**	**81.41**	**57.11**	**84.83**	**66.35**	**80.22**	**50.10**	**85.54**	**59.67**	**83.00**
	CR	w/o E_p	65.77	80.43	65.84	80.40	66.89	79.64	**55.38**	82.82	63.47	80.82
		w/ E_p	**61.81**	**81.81**	**59.14**	**82.58**	**66.83**	**80.32**	58.12	**83.47**	**61.48**	**82.05**
NFC	CNR	w/o E_p	74.78	69.01	71.68	68.11	76.62	62.96	64.30	72.62	71.85	68.18
		w/ E_p	**70.93**	**70.45**	**68.04**	**71.62**	**56.85**	**74.44**	**57.30**	**74.41**	**63.28**	**72.73**
	CR	w/o E_p	73.31	69.55	72.90	76.77	59.12	71.08	72.34	71.09	69.42	72.12
		w/ E_p	**67.04**	**71.97**	**58.29**	**78.11**	**57.34**	**73.37**	**49.22**	**79.51**	**57.97**	**75.74**
DAC	CNR	w/o E_p	55.72	82.28	71.86	75.53	**52.35**	75.33	71.49	74.94	62.86	77.02
		w/ E_p	**55.13**	**82.33**	**52.97**	**77.33**	52.36	**75.38**	**55.94**	**75.00**	**54.10**	**77.51**
	CR	w/o E_p	53.55	83.55	69.02	76.69	52.12	75.58	49.90	78.50	56.15	78.58
		w/ E_p	**52.24**	**84.03**	**58.59**	**76.90**	**51.63**	**76.90**	**48.67**	**80.00**	**52.78**	**79.46**

B.1 Impact of Trajectory Probability Energy

Table 6 compares performance with and without the inclusion of trajectory probability energy (E_p) across various models and evaluation scenarios. The results demonstrate that incorporating E_p consistently enhances performance across all metrics (FPR95 and AUROC), as evidenced by lower FPR95 values and higher AUROC scores. The improvements are particularly significant in the OOD and NFC evaluations, where E_p significantly reduces FPR95 and increases AUROC, especially for models such as PlanTF and PlanScope.

Table 7: Detailed results of the ablation study on Gaussian Fourier Projection (GFP).

Mode	Module	PlanTF		PLUTO		GameFormer		PlanScope		Average	
		FPR95 ↓	AUROC ↑	FPR95 ↓	AUROC ↑	FPR95 ↓	AUROC ↑	FPR95 ↓	AUROC ↑	FPR95 ↓	AUROC ↑
OP	w/o GFP	69.34	82.23	56.42	83.20	65.32	80.30	**55.58**	85.77	61.67	82.88
	w/ GFP	**51.02**	**84.48**	**53.54**	**85.50**	**59.59**	**84.82**	56.18	**85.83**	**55.08**	**85.16**
CNR	w/o GFP	**63.88**	80.73	62.87	82.15	66.69	**80.23**	57.25	85.49	62.67	82.15
	w/ GFP	65.11	**81.41**	**57.11**	**84.83**	**66.35**	80.22	**50.10**	**85.54**	**59.67**	**83.00**
CR	w/o GFP	65.74	79.10	65.20	81.54	**56.85**	**80.72**	66.94	82.13	63.68	80.87
	w/ GFP	**61.81**	**81.81**	**59.14**	**82.58**	66.83	80.32	**58.12**	**83.47**	**61.48**	**82.05**

B.2 Impact of Gaussian Fourier Projection

Table 7 presents a comparison of OOD detection performance before and after removing the Gaussian Fourier Projection (GFP) in the velocity field module of flow matching. The results indicate that incorporating the GFP improves the overall OOD detection performance across all four planners.

Table 8: Detailed results of the ablation study on Gaussian Mixture Model (GMM).

Mode	Module	PlanTF		PLUTO		GameFormer		PlanScope		Average	
		FPR95 ↓	AUROC ↑	FPR95 ↓	AUROC ↑	FPR95 ↓	AUROC ↑	FPR95 ↓	AUROC ↑	FPR95 ↓	AUROC ↑
OP	w/o GMM	62.05	82.55	63.21	**85.73**	62.66	83.64	56.53	85.76	61.11	84.42
	w/ GMM	**51.02**	**84.48**	**53.54**	85.50	**59.59**	**84.82**	**56.18**	**85.83**	**55.08**	**85.16**
CNR	w/o GMM	67.56	81.08	**55.72**	**85.31**	**62.76**	80.17	60.66	84.59	61.68	82.79
	w/ GMM	**65.11**	**81.41**	57.11	84.83	66.35	**80.22**	**50.10**	**85.54**	**59.67**	**83.00**
CR	w/o GMM	75.45	73.64	71.38	73.97	**62.80**	**80.36**	71.70	73.86	70.33	75.46
	w/ GMM	**61.81**	**81.81**	**59.14**	**82.58**	66.83	80.32	**58.12**	**83.47**	**61.48**	**82.05**

B.3 Impact of Gaussian Mixture Model Prior

Table 8 presents a comparison of OOD detection performance before and after replacing the Gaussian Mixture Model (GMM) with a standard distribution. The results indicate that GMM prior distribution is more effective.

Table 9: Inference time of REDOUBT on different motion planners.

Planner	PlanTF	PLUTO	GameFormer	PlanScope
Inf. Time	3.12 ms	3.30 ms	10.79 ms	3.25 ms

Figure 4: Ablation study on λ: (a) OOD Detection (OP Mode), (b) NFC Estimation (CNR Mode), and (c) DAC Estimation (CNR Mode).

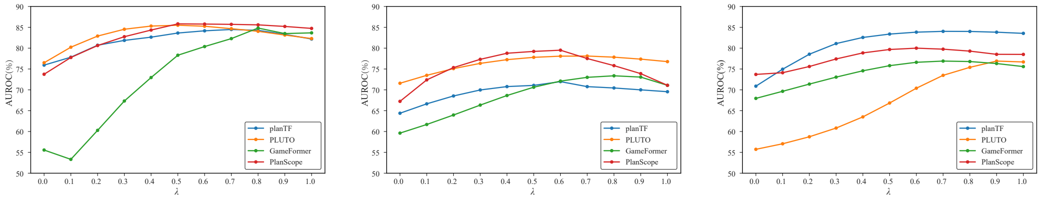

(a) OOD Detection (OP Mode)

(b) NFC Estimation (CNR Mode)

(c) DAC Estimation (CNR Mode)

B.4 Hyperparameter Sensitivity

Figure 4 contains three subfigures illustrating performance trends for OOD detection under the OP mode, NFC estimation, and DAC estimation under the CNR mode. Each subfigure shows the performance of various planners as λ varies from 0 to 1, where $\lambda = 0$ represents the configuration without Flow Matching, and $\lambda = 1$ represents the configuration without E_p. The results indicate that the optimal range for λ lies between 0.5 and 0.8. For example, OOD detection with $\lambda = 0.8$ achieves the optimal performance for GameFormer. The hyperparameter averages the strengths of both methods, avoiding the shortcomings of relying exclusively on one.

C Inference Time

Table 9 illustrates the inference time of REDOUBT on different motion planners. REDOUBT introduces an additional inference time of only 3.12 to 10.79 ms. Considering that the original planner operates at 20 Hz (resulting in a latency of 50 ms per frame), the extra latency from REDOUBT is minimal. Importantly, the total latency remains well below the maximum threshold of 1000 ms per inference mandated by the nuPlan benchmark [17]. These results demonstrate that REDOUBT is computationally efficient and capable of meeting the real-time performance requirements of modern motion planners.

D Limitations

We use nuPlan for validation because it is currently the only large-scale dataset specifically designed for motion planning, offering both open-loop and closed-loop evaluation settings. Most existing ML-based motion planners [22, 8, 46, 7]are exclusively trained and tested on nuPlan due to the lack of other comparable motion planning datasets. We recognize that further validation on additional datasets would enhance the generalizability of our framework, and we aim to include them in the future when new datasets become publicly available.

E Broader Impacts

This paper presents REDOUBT, a novel duo safety validation framework for motion planning in autonomous driving. Autonomous driving is a safety-critical domain where rigorous safety validation is crucial to prevent potentially hazardous decisions. REDOUBT is the first systematic safety validation framework that employs a duo mechanism to simultaneously inspect both input distributions and output uncertainty. This dual inspection approach reveals two previously overlooked unsafe scenarios arising from the interplay between InD/OOD inputs and certain/uncertain planning decisions.

To address these scenarios, we propose two specialized solutions: (1) OOD detection using latent flow matching, and (2) decision uncertainty estimation via an energy-based approach. Extensive experiments demonstrate that both modules significantly outperform existing methods under both open-loop and closed-loop evaluation settings. By improving the safety and reliability of autonomous driving systems, REDOUBT offers broad applicability across industries, contributing to safer and more dependable autonomous vehicles.

Notably, several leading autonomous driving companies, such as Momenta [5], have already adopted learning-based planners in their systems. Our method is well-suited for such deployments, as it integrates seamlessly into the pipeline. Specifically, the input to our method would be the latent space representation from the autonomous driving stack, and the output would include whether it represents an OOD scenario and risk probabilities of potential driving violations.

Several practical challenges need to be addressed for real-world deployment. Our approach could identify more unsafe scenarios than traditional methods. This raises the question of how to balance sensitivity and specificity in decision making [21]. To address these challenges, we propose that the output of our method serves as helpful, supplementary information to existing decision-making mechanisms within the stack. For instance, it could integrate with existing systems to trigger takeover requests as needed. Additionally, our system could be optionally enabled to prioritize safety in specific scenarios, such as high-risk environments or areas prone to OOD events.